Proc. IEEE Int. Conf. on Robotics and Automation (ICRA 2013), Karlsruhe, Germany, pp. 376-381, IEEE 2013

Prediction of Human Collision Avoidance Behavior by Lifelong Learning for Socially Compliant Robot Navigation

Christoph Weinrich, Michael Volkhardt, Erik Einhorn and Horst-Michael Gross

Abstract— **In order to act socially compliant with humans, mobile robots need to show several behaviors that require the prediction of people's motion. For example, when a robot avoids a person, it needs to respect the human's personal space [1] and the avoidance behavior needs to be smooth, so that it is understandable to the interaction partner. To achieve this, the robot needs to reason about future paths a person is likely to follow. Because humans adapt their avoidance behavior to the robot's motion, the proposed method performs lifelong learning of the people's behavior while it adapts its own behavior to their motion. The human avoidance behavior is modeled by a discrete, multi-modal, spatio-temporal distribution over the people's future occurrences. This prediction is based on the people's positions and their velocities relatively to the robot and the obstacle situation of the robot's environment. The proposed prediction method is significantly better than a simple linear prediction. Particularly, for tactical decisions, like whether to avoid a moving person on the left or on the right side, this approach is well suited. Furthermore, when the humans get used to a robot, also a long-term change of the human behavior towards the robot can be learned by our approach.**

I. INTRODUCTION

For mobile service robots, the navigation has not only instrumental function to accomplish the robot's tasks. Especially in public, sometimes crowded environments, like supermarkets or home improvement stores, the navigation is also part of nonverbal communication and has socio-emotional importance. To optimize the human-robot interaction (HRI), it is necessary that the robot's navigation behavior is socially acceptable for the users of the robot and for uninvolved bystanders, likewise. Particularly, assistant or guiding robots need to be comprehensible, kind, and non-intrusive. The application area of our robot is a home improvement store. The robot's task is to guide customers to goods they are looking for. As one result of long-term field trials executed in 2008 and 2009 [2], the following three behaviors appeared important within this scenario:

Polite approaching: When a robot recognizes a person willing to interact with the robot, it should approach the person in a socially acceptable manner. The approached human feels more comfortable when the robot shows an approach behavior [3] where certain distances are kept [4].

Person focused guiding: When a robot guides a person, e.g. through a home improvement store, it should adapt its speed depending on the distance to the person, so that the person can follow comfortably.

This work has received funding from the Ph.D. Graduate School on Image Processing and Image Interpretation at Ilmenau University of Technology.

All authors are with Neuroinformatics and Cognitive Robotics Lab, Ilmenau University of Technology, 98694 Ilmenau, Germany christoph.weinrich at tu-ilmenau.de

Regardful navigation: During navigation, mobile robots have to pass or avoid bystanders who are not interested in an active interaction with the robot. Thereby, the navigation should conform to the proxemics [1] again.

These three behaviors are essentially influenced by the humans' motion relative to the robot. To achieve a smooth transition during the execution of these behaviors and thereby to improve understandability for the humans, the robot needs to reason about future paths the humans are likely to follow. From our own experiments and literature we know that the human motion towards other humans differs from the motion towards robots. Hence, typical human motion patterns can not be learned from human-human interaction. In fact, the humans' paths depend on the robot's appearance and its behavior [5], [6]. Therefore, our approach learns how humans move in the presence of our robot by observing the humans during its operation.

Although the proposed prediction method can be used for all three behaviors, we will refer to the regardful navigation in this paper. Essentially, our robot respects the personal space [1] around humans while it avoids them or gives way. Particularly, when a human and a robot avoid each other, each of them needs to anticipate the other's motion and adapt its own behavior accordingly. While the robot learns how humans avoid it and uses this prediction to avoid the humans, it adapts its behavior towards the human. The human motion, in turn, is influenced by the robots actions. Considering this feedback loop, the robot performs lifelong learning of the human avoidance behavior, while it continuously adapts its own behavior.

The prediction of the humans' motion is based on their relative position to the robot, the human's velocity vector, and a sparse coding of the current obstacle situation in their environment. In contrast to related work (Sec. II) for human motion prediction, we are interested in short-term prediction of the human motion while the human and the robot are avoiding each other. The global position of a person becomes less important than the spatial relation between human and robot. This allows us to use a relative representation of the person position in the state space, resulting in a better coverage with training data and a better generalization for changing environments.

The next section reviews related work in the field of human motion prediction. Afterwards, Sec. III describes how humans are tracked and their future occurrences are predicted in our approach. Sec. IV describes how these predictions are integrated within the Dynamic Window Approach [7] to obtain a regardful navigation behavior. Thereafter, in Sec. V

the prediction quality and measurable advantages for humans are evaluated.

II. RELATED WORK

Many methods for avoiding [8], [9] or approaching [10] humans by mobile robots integrate typical motion patterns of humans into the robot's path planning algorithm. For example, in [8] stationary laser-range finders are used to capture motion patterns of humans within an office environment. A Hidden Markov Model is trained on this data and applied to predict future positions of detected people. The predicted trajectories are used during global path planning by the A* algorithm on a 3D time-space cost map.

However, these approaches do not generalize for changes in the environment. Therefore, in [11] the goal-directed trajectories of pedestrians are modeled using inverse reinforcement learning. The learned cost functions generalize for changes in the environment or even entirely different environments. During path planning with the D* algorithm, the time-varying predictions are added as costs to the cost map. However, for this approach the pededstrians' prior probability distributions over global target positions are required. Therefore, the persons' trajectories within the robot's operational environment are tracked with external laser scanners.

The intention of the above mentioned approaches is to predict the humans' motion already when the robot is far away. Then the predictions are used to spaciously avoid the humans, preferably not influencing their trajectories by the robot's presence. However, in crowded environments it is almost impossible for the robot to reach its goal if the robot does not consider that the people will avoid it. In [12] this is called the "freezing robot problem". The proposed solution is a direct interaction of human and robot, where the robot acts socially compliant while human and robot engage in joint collision avoidance. Accordingly, in [13] the basic idea of feature matching using maximum entropy distributions [11], is used to model the cooperation of multiple people. This model is used to predict the trajectories of the humans and the robot based on their current positions. Then, the robot follows the trajectory which was predicted for itself. However, like in [11], the humans' global target positions need to be estimated.

Furthermore, it is noted in [12], [13] that humans react differently to robots than to other humans. Therefore, models which are learned from human-human interaction, like the social forces model [14], relative motion prototypes [15] or inverese reinforcement learning [16], are not directly transferable to human-robot interaction. In contrast to the above mentioned methods, training data needs to be captured while the robot is actually present. In this case, the robot is able to capture the training data, and the operational area does not need to be equipped with an external tracking system, like laser-range finders, which were used for many of the aforementioned approaches. Because humans are only locally avoided, the time of avoidance and the necessary prediction time reduces, resulting in generally less uncertainties.

III. PERSON TRACKING AND PREDICTION

A. Person Tracking

The positions of people are tracked by the robot using a Kalman filter-based tracking system. The system applies visual person detection and upper body orientation estimation [17] based on Histograms of Oriented Gradient (HOG) features [18]. An additional cue is given by laser-range finder-based boosted leg detection [19]. The Kalman filter tracks person hypotheses in a nine-dimensional state space in which position, velocity, and orientation of the person are represented by 3 dimensions, respectively.

For the human motion prediction, we are only interested in the position and velocity of persons in the xy-plane. Therefore, the system generates a person specific track for each hypothesis $\mathbf{s}_i(t) = (\mathbf{p}_i(t), \mathbf{v}_i(t))$ for each time step t, where $\mathbf{p}_i(t)$ denotes the person's 2D position, $\mathbf{v}_i(t)$ denotes the 2D velocity and i is the identification number of the respective track. Note, that position and velocity are given relatively to the current robot position $\mathbf{r}(t)$. The robot's velocity might be added to the state space to improve the prediction, but this increase of dimensionality is not investigated in this paper.

B. Human Motion Prediction

For prediction of the future person positions, the person's state $\mathbf{s}_i(t)$ is complemented by the obstacle situation in the robots environment $\mathbf{e}(t)$. The obstacle situation $\mathbf{e}(t)$ is coded by a 3D vector, whereas each dimension represents the average distance of a 90° section (left, front, right) of the 270° laser scan. This results in a seven dimensional state space $\mathbf{s}_i(t) = (\mathbf{p}_i(t), \mathbf{v}_i(t), \mathbf{e}(t))$. An on-line clustering function $c(\mathbf{s}_i(t)) = c_j$ is used to iteratively form C clusters from all observed states $\mathbf{s}_i(t)$ in state space S. As shown in Fig. 1, for each cluster c_j a spatio-temporal belief distribution is stored in terms of a set of belief distribution grid maps $\mathbf{M}_1^{c_j}, \ldots, \mathbf{M}_T^{c_j}$. The cells of each map $\mathbf{M}_\tau^{c_j}$ represent the belief $Bel(c_j, \Delta t_\tau, x, y)$ of the expected person's position (x, y) relatively to the current robot position $\mathbf{r}(t)$ in a future time interval Δt_τ.

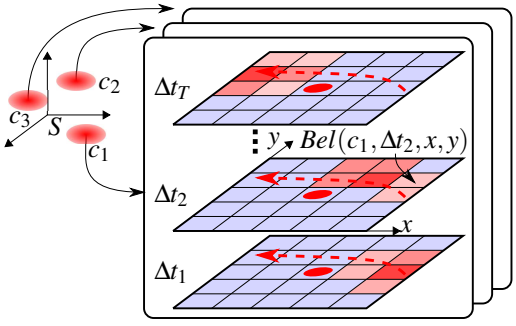

Fig. 1. Each cluster c within the seven-dimensional state space S holds a discrete, multi-modal belief distribution map over the future person positions for multipe prediction time intervals Δt. The positions of the grid cells are relative to the initial robot position $\mathbf{r}(t)$ at the time of prediction. Accordingly, the robot's initial position $\mathbf{r}(t)$, which is marked by a red ellipse, is always located in the center of the belief maps. The dashed arrow shows the motion of the maximum belief, which is visualized by the intensity of the red color, over time.

While the robot interacts with humans, each tracked person hypothesis is mapped to the state space yielding

the current state $\mathbf{s}_i(t)$. Then, $\mathbf{s}_i(t)$ is used to update the position of the best matching cluster $c(\mathbf{s}_i(t))$ according to a sequential implementation of the k-means algorithm [20], using the normalized Euclidean distance as distance measure. Furthermore, the current person position $\mathbf{p}_i(t)$ is used to update the belief distribution maps of previous best matching clusters $c(\mathbf{s}_i(t-\Delta t_1)), c(\mathbf{s}_i(t-\Delta t_2)), \ldots, c(\mathbf{s}_i(t-\Delta t_T))$. For each previous best matching cluster $c(\mathbf{s}_i(t-\Delta t_\tau))$ at time $t-\Delta t_\tau$ the current person position $\mathbf{p}_i(t)$ is transformed relatively to the previous robot position $\mathbf{r}(t-\Delta t_\tau)$. The belief distribution of the cluster is finally updated by incrementing the belief value of the cell in map $\mathbf{M}_\tau^{c(\mathbf{s}_i(t-\Delta t_\tau))}$ that corresponds to that relative person position. Hence, the current person position acts as prediction for the past point of time $t-\Delta t_\tau$.

IV. REGARDFUL NAVIGATION

To obtain a regardful navigation behavior, the predicted spatio-temporal occupation probabilities of the tracked people are respected during planning of the robot's motions. This is performed by the "regardful navigation objective", an additional objective rating candidate motion commands in the dynamic window approach (DWA) [7]. The physically possible velocities, which are achievable by the according motor commands, are sampled. For each velocity $\mathbf{v}$, a cost value $cost(\mathbf{v})$ is calculated, which specifies the probability that the robot will collide with the personal spaces of the tracked persons within the prediction window Δt. The prediction time varies between 2 and 5 seconds, depending on the robot's velocity. Therefore, for each currently tracked person i the considered time window is sampled T times to find the maximum violation of the person's personal spaces at a future point of time by the future robot position. Then, the maximum violation costs of all persons are averaged:

$$cost(\mathbf{v}) = \frac{1}{i}\sum_i \max_{\Delta t_1,\cdots,\Delta t_T} F(\underbrace{\mathbf{r}(t)+\mathbf{v}\cdot\Delta t}_{\mathbf{r}'=\mathbf{r}(t+\Delta t)}, t, \Delta t, i) \qquad (1)$$

The cost function F predicts the violation costs of the personal space of a person i at time $t+\Delta t$ by the robot at its future position $\mathbf{r}(t+\Delta t)$. The future robot position results from the robot's velocity $\mathbf{v}$ and the prediction time Δt. A simple cost function F_l linearly predicts the future person position and represents the violation costs of its personal space by a Gaussian function:

$$F_l(\mathbf{r}', t, \Delta t, i) = \exp\left(-\frac{|\mathbf{r}' - (\mathbf{p}_i(t)+\mathbf{v}_i(t)\cdot\Delta t)|}{2\sigma^2}\right) \qquad (2)$$

This simple cost function is presented here, because it is used during our experiments to benchmark a more sophisticated cost function F_p, which uses the learned belief distribution maps to predict the future person positions:

$$F_p(\mathbf{r}', t, \Delta t, i) = \sum_{x,y} \exp\left(-\frac{|\mathbf{r}' - (x,y)^T|}{2\sigma^2}\right) \cdot \frac{Bel(c(\mathbf{s}_i(t)), \Delta t, x, y)}{\sum_{x,y} Bel(c(\mathbf{s}_i(t)), \Delta t, x, y)} \qquad (3)$$

The cost function $F_p(\mathbf{r}', t, \Delta t, i)$ of a certain cluster $c_j = c(\mathbf{s}_i)$ is visualized in Fig. 2. For each time interval Δt, a continuous cost function for violation of the person's anticipated personal space is coded by a Mixture of Gaussians. Therefore, a Gaussian function is placed at each grid cell $(x,y)^T$ of the belief distribution map, and each Gaussian is scaled with the belief $Bel(c_j, \Delta t, x, y)$ of the cell. Then, the given robot velocity $\mathbf{v}$ (green arrow) is used to calculate the future robot position $\mathbf{r}(t+\Delta t) = \mathbf{r}(t) + \mathbf{v}\cdot\Delta t$ (green ellipse) relatively to the current robot position $\mathbf{r}(t)$ (red ellipse). The costs of a velocity $\mathbf{v}$ result from the value of the mixture of Gaussian function at the future robot position $\mathbf{r}' = \mathbf{r}(t+\Delta t)$.

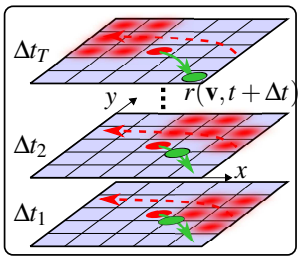

Fig. 2. Cost value calculation for a given cluster c_j and robot velocity $\mathbf{v}$ (green arrow) for different time intervals Δt: At each grid cell (x,y) a two-dimensional Gaussian function represents the costs for entering the personal space of a person located at the cells center. Each Gaussian function is scaled by the belief $Bel(c_j, \Delta t, x, y)$ (see Fig. 1) that a person will be at this position at Δt. The costs of a future robot position $\mathbf{r}(\mathbf{v}, t+\Delta t)$ result from the value of this mixture of Gaussian function at the future robot position.

One parameter of the cost calculation functions F_l and F_p is the standard deviation σ of the applied Gaussian function. It influences the size of the personal space around the detected people and, thereby, how respectful the "regardful navigation objective" behaves. Furthermore, the robot's politeness is also dependent on the weight of this objective compared to the weights of the other objectives within the DWA. As noted in [12], a robot could learn that humans always give way when the robot aggressively approaches them. Accordingly, it is not enough if the robot predicts the human motion correctly. Instead of that, the robot needs to keep enough distance that the person does not hesitate to choose a more pleasent path. Accordingly, in the next section the prediction accuracy and the degree of the robots politeness are investigated separately.

V. EXPERIMENTS

To analyze the abilities of our approach, we performed several experiments, separated into analysis of the motion prediction on its own and the actual influence of the obtained robot behavior to the human motion. These experiments were performed in a hallway of an office building (Fig. 3).

A. Prediction accuracy

The first experiment was supposed to validate whether the belief distribution maps are generally suitable to predict the human motion. Therefore, the quality of the cost function $F_p(\mathbf{r}', t, \Delta t, i)$, which is based on the predicted belief distribution maps, is compared with a simple cost function $F_l(\mathbf{v}, \Delta t, i)$, which is based on linear prediction of the human

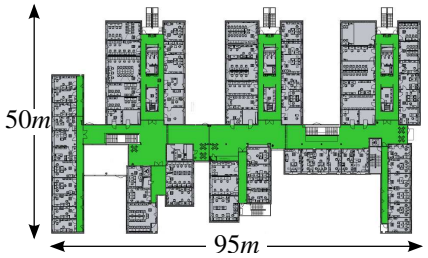

Fig. 3. One floor of the office building where the experiments were performed. The operational area of the guide robot is highlighted green.

motion. The used quality criterion is the continuous cross-correlation cc_F of the predicted cost function $F(\mathbf{r}',t,\Delta t,i)$ and a ground-truth cost function $G(\mathbf{r}',t+\Delta t,i)$, which is based on a subsequent observation of the actual person position at time $t' = t+\Delta t$:

$$cc_F(t,\Delta t,i) = \int_{\mathbf{r}\in\mathbb{R}^2} F(\mathbf{r}',t,\Delta t,i)\cdot G(\mathbf{r}',t+\Delta t,i)\,dr \quad (4)$$

$$G(\mathbf{r}',t',i) = \exp\left(-\frac{|\mathbf{r}'-\mathbf{p}_i(t')|}{2\sigma^2}\right) \quad (5)$$

The evaluation of the cost functions is suitable for the continuous linear prediction that is used for F_l and the predicted discrete distribution that is used for F_p. Furthermore, the cost functions are evaluated, because they directly influence the robot's regardful navigation behavior. Certainly, the cost functions (Eq. 2, 3, 5) depend on the used standard deviation σ. Therefore, different standard deviations have been investigated.

Fig. 4. Robot's path (blue) within the hallway. The tracked paths of the people in the robot's environment are shown in red color. The tracked person positions were firstly used for online evaluation of the prior trained motion model and thereafter to train the motion model for later evaluation.

For this experiment, the robot visited different navigation points at the main floor, using the E* algorithm [21] for global path planning. During its tour, people were tracked and their states $\mathbf{s}_i(t)$ were used to predict the future cost functions using $F_p(\mathbf{r}',t,\Delta t,i)$ and $F_l(\mathbf{r}',t,\Delta t,i)$. Furthermore, the posterior observed states $\mathbf{s}_i(t+\Delta t)$ were used for the cost function $G(\mathbf{r}',t+\Delta t,i)$ and to update the belief distribution maps. Note, that during this first experiment the cost function $F_l(\mathbf{r}',t,\Delta t,i)$ has been used for regardful navigation. This is to make sure that the robot does not change its behavior during learning of the human motion, because this might in turn effect the learned human motion. The robot's path during this experiment is shown in Fig. 4 with blue color. The persons' tracks, which were used to train and evaluate the predictions, are shown in red color.

Fig. 5 visualizes the belief grid maps of a trained cluster. Altogether 600 clusters were used, and for each of them 20 belief distribution maps were learned, with each map

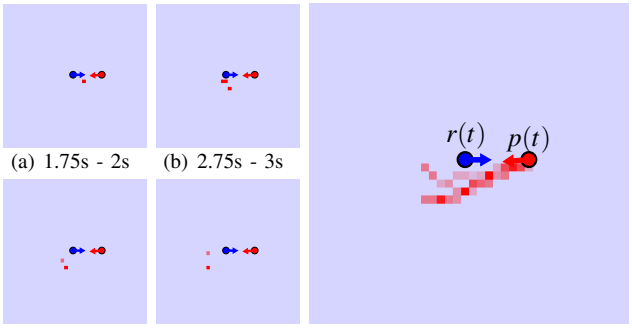

(a) 1.75s - 2s (b) 2.75s - 3s (c) 3.75s - 4s (d) 4.75s - 5s (e) 0s - 5s

Fig. 5. Visualization of one cluster's trained belief distribution maps of future person positions (see schematic diagram in Fig. 1). The cluster's initial person position and velocity (red arrow) is considered relatively to the initial robot pose (blue arrow). Each belief distribution map covers a $250ms$ interval in time and $15m \times 15m$ in space with 40×40 grid cells. For each grid cell, the belief is coded by the intensity of the red color: a)-d) 4 of 20 individual belief distribution maps e) belief distribution over all intervals from 0s to 5s accumulated

storing the belief over a 250ms interval, resulting in a total prediction window of 5 seconds. Each grid map covers $15m \times 15m = 225m^2$ of the robot's local surroundings using $40 \times 40 = 1600$ grid cells. Using floating point precision to store the belief, overall around 74MB were necessary to store all belief distribution maps of all clusters. Admittedly, an intensive examination of the number of neccessary clusters should be made or an incremental cluster approach should be applied in future.

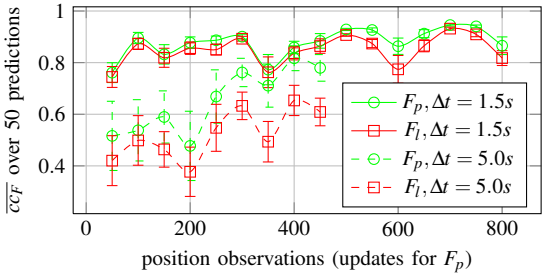

(a) $\sigma = 1.0m$

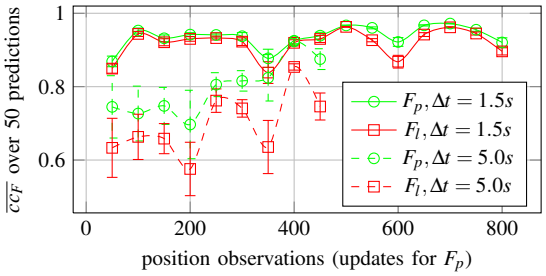

(b) $\sigma = 2.0m$

Fig. 6. Evaluation of linear predicted cost function F_l and cost function F_p, which is based on our proposed motion model. Both cost functions were evaluated by cross correlation cc_F with the ground-truth cost function G, whereas in a) a standard deviation $\sigma = 1.0m$ and in b) $\sigma = 2.0m$ was used. Each plot is low-pass filtered by averaging over 50 consecutive cross correlation values. There are less position observations for 5s prediciton than for 1.5s, because the on-board tracker could not always track the persons complete 5s.

Fig. 6 visualizes the prediction quality of the proposed approach F_p (solid graphs) and the linearly predicted cost

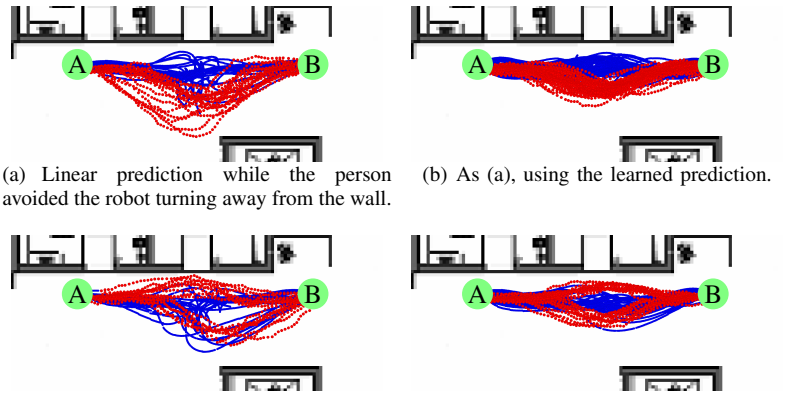

(a) Linear prediction while the person avoided the robot turning away from the wall.

(b) As (a), using the learned prediction.

(c) Linear prediction while the person avoided the robot according to right-hand traffic rules.

(d) As (c), using the learned prediction.

Fig. 7. Robot's path (blue) and human path (red) during mutual avoidance while person and robot repeatedly swapped positions A and B. In a),b) the person avoided the robot always turning away from the wall. In c),d) the person avoided the robot according to right-hand traffic rules.

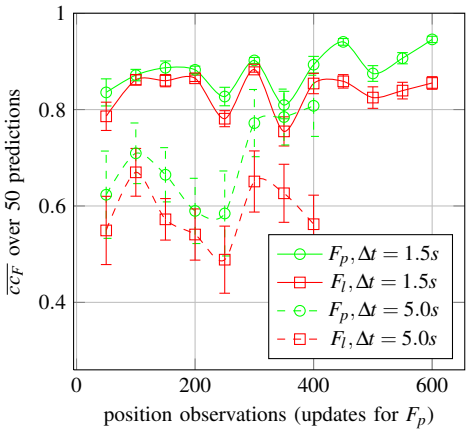

Fig. 8. Evaluation of linear predicted cost function F_l and cost function F_p, which is based on our proposed prediction method. Particularly, for the 5.0s prediction the improvement by the learning approach compared to the linear prediction becomes evident.

function F_l (dashed graphs). Note, that the cross correlation of an equally distributed belief would be around 0.055 and the maximum reachable cross correlation is 1.0. After 50 predictions of a certain prediction window Δt have been validated, the average cross correlation value $\overline{cc_F}$ over the last 50 evaluations is plotted. It is shown that the proposed approach F_p always gains a better $\overline{cc_F}$ than the linear method. Furthermore, it is shown that the difference between both approaches increases, because F_p improves due to learning and F_l is static. This is particularly evident for the 5 seconds prediction interval. The use of different standard deviations in Fig. 6(a) and Fig. 6(b) shows that a bigger σ generally supports the cross correlation, but does not induce a qualitative difference. Note, that the applied Kalman filter-based tracker uses a linear prediction model. Thereby, whenever persons were not detected properly, the linear predicted cost function F_l profits. Furthermore, many persons were tracked in great distance to the robot. Thereby, the robot often had very little influence on the people's path, and the people could continue their mostly linear path. However, particularly when person and robot are very close to each other, the prediction becomes important because both have to deviate from a straight-lined path. This is investigated in the next experiment.

B. Detour of humans during robot avoidance

In this experiment, the actual influence of the human motion modeling on the robot behavior is investigated. Obviously, the satisfaction of the robot's interaction partners with the robot's behavior would be a particularly suitable quality criterion. However, at the moment technically measurable quality criteria are used. Taking into account that humans prefer to walk economically, we used the people's detour during robot avoidance to benchmark the robot's behaviors.

Therefore, we created a setup where a person and the robot repeatedly had to swap positions, whereby they were forced to pass each other (Fig. 7). Thereby, two different avoidance behaviors were performed and for each behavior the linear predicted cost function F_l and the proposed cost function F_p were tested. During two experiments, the person avoided the robot at the side with the greatest clearance (Fig. 7(a) and 7(b). The "greatest clearance avoidance" corresponds to a careful behavior, which expects little abilities of the robot. During the third 7(c) and fourth 7(d) experiment, the person avoided the robot according to right-hand traffic rules. This means that the person had to walk between robot and wall, when moving from starting position B to goal position A. Initially, the robot's belief distribution maps were untrained. Thus, the robot had to learn the humans' avoiding strategy and adapt its behavior while the experiment was performed.

The prediction accuracy for the second experiment is visualized in Fig. 8. It shows that F_l is insufficient to model this nonlinear avoidance behavior. In contrast, F_p continuously improves while on-line learning compared to F_l. Note, that the robots behavior and therewith the human avoidance strategy changes while the robot learns the human motion. The actual impact to the robot's motion and thereby to the human avoidance becomes clear, when the human detour is evaluated.

Although the robot uses its laser-range finder for obstacle detection and person tracking, the evaluation is based on an external tracking system [22], delivering ground truth data independent of potential error in the robot's self localization or person tracking system. While the person and the robot avoided each other, the detour of the human relatively to the direct connection of starting point and end point was captured. The visualization of the paths is shown in Fig. 7 and the results of the avoidance detour calculation are presented in Fig. 9.

For both avoiding strategies, during training of the proposed prediciton function F_p, the detour decreases steadily and reaches lowest values compared to avoidance, which is based on linear predicition F_l or without prediction F_n. Further below is explained, why the linear prediciton causes the robot to avoid in the same direction as the person. Since no avoidance would be better in this case, the plot for F_n in Fig. 9 additionally shows the detour, when the robot assumes that the person stays where it is currently observed. Notice, that the detour decreases when linear prediciton is used,

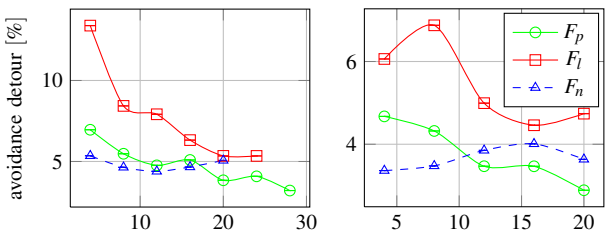

Fig. 9. Human detour for clearance directed (a) and right-hand traffic (b) avoidance. For both strategies the progress of the detour when using linear prediciton F_l, proposed prediciton F_p and no prediciton F_n are plotted. Each plot is low-pass filtered by averaging over 4 consecutive detour values.

although the linear prediction does not learn. Instead, the person learned to avoid the robot early, to prevent it from avoiding in the same direction. During "clearance directed avoidance" the robot had to avoid the person towards the wall when moving from A to B and vice versa. During "right-hand traffic avoidance" the robot only had to avoid the person towards the wall when moving from B to A. Because the wall limits the robot's avoidance space, the human avoidance detour is greater for the "clearance directed avoidance". When the robot uses linear prediction for the cost function F_l, it tends to avoid the person turning away from the wall. This is because next to the "regardful navigation objective" a "distance objective" is used for the "dynamic window approach" [7]. This objective calculates greater costs $cost(v)$ for velocities, which lead towards the wall. When the person applied "right-hand traffic" and walked from B to A, person and robot perfectly avoided each other. But when the person walked from A to B or when the person applied the "biggest clearance avoidance", the person and the robot tried to avoid each other at the same side. Thereby, the robot even had to back up sometimes. This is the reason why the linear prediction causes particularly long avoidance detour for humans which apply the "clearance directed avoidance".

VI. CONCLUSIONS

This paper addresses the joint collision avoidance of humans and robots. Instead of global prediction of human motion and spaciously avoidance of the tracked people, they are avoided locally in a socially compliant manner. Thereby the human motion is directly influenced by the robot's presence and its navigation behavior. Therefore, we propose a method for lifelong learning of the human motion in proximity to a robot. The motion prediction is based on the person's position and velocity relatively to the robot and the obstacle situation in their local environment. We have shown that belief distribution maps are suitable to learn and predict human motion within a large hallway environment. Furthermore, these predictions are efficiently integrable into the DWA for motion planning respecting the human personal space. Our experiments show that particularly the correct prediction of the person's avoidance direction of the robot has great influence on the joint collision avoidance. In contrast to linear prediction, our proposed method could anticipate the direction of avoidance correctly for different avoidance strategies. Thereby, the human avoidance detour during the avoidance maneuver is significantly lower.

The proposed approach is able to predict the motion of several persons and to respect their personal space. However, the motion prediction does not explicitly consider the interactions of these persons among each other. Accordingly, we plan to extend the proposed approach in future work. Furthermore, we plan to socially evaluate the robot behavior.

REFERENCES

[1] E. T. Hall, "A system for the notation of proxemic behavior," *American Anthropologist*, vol. 65, no. 5, pp. 1003–1026, 1963.
[2] Gross et al., "TOOMAS: Interactive shopping guide robots in everyday use - final implementation and experiences from long-term field trials," in *Proc. Int. Conf. on Intel. Robots and Systems*, 2009, pp. 2005–2012.
[3] M. Svenstrup, S. Tranberg, H. Andersen, and T. Bak, "Pose estimation and adaptive robot behaviour for human-robot interaction," in *Proc. of Int. Conf. on Robotics and Automation (ICRA)*, 2009, pp. 3571–3576.
[4] Dautenhahn et al., "How may i serve you?: a robot companion approaching a seated person in a helping context," in *Proc. of Int. Conf. on Human-Robot Interaction (HRI)*, 2006, pp. 172–179.
[5] M. Walters, M. Oskoei, D. Syrdal, and K. Dautenhahn, "A long-term human-robot proxemic study," in *Proc. of Int. Symp. on Robot and Human Interactive Communication (RO-MAN)*, 2011, pp. 137–142.
[6] H. Huettenrauch, K. Eklundh, A. Green, and E. Topp, "Investigating spatial relationships in human-robot interaction," in *Proc. Int. Conf. on Intelligent Robots and Systems (IROS)*, 2006, pp. 5052 –5059.
[7] D. Fox, W. Burgard, and S. Thrun, "The dynamic window approach to collision avoidance," *Robotics & Automation Magazine, IEEE*, vol. 4, no. 1, pp. 23–33, Mar 1997.
[8] M. Bennewitz, W. Burgard, G. Cielniak, and S. Thrun, "Learning motion patterns of people for compliant robot motion," *International Journal of Robotics Research*, vol. 24, no. 1, pp. 1–30, 2005.
[9] Thompson et al., "A probabilistic model of human motion and navigation intent for mobile robot path planning," in *Proc. of 4th Int. Conf. on Autonomous Robots and Agents (ICARA)*, 2009, pp. 663 –668.
[10] Satake et al., "How to approach humans?: Strategies for social robots to initiate interaction," in *Proc. of Int. Conf. on Human Robot Interaction (HRI)*, 2009, pp. 109–116.
[11] Ziebart et al., "Planning-based prediction for pedestrians," in *Proc. of Int. Conf. on Intel. Robots and Systems (IROS)*, 2009, pp. 3931 –3936.
[12] P. Trautman and A. Krause, "Unfreezing the robot: Navigation in dense, interacting crowds," in *Proc. of Int. Conf. on Intelligent Robots and Systems (IROS)*, oct. 2010, pp. 797 –803.
[13] M. Kuderer, H. Kretzschmar, C. Sprunk, and W. Burgard, "Feature-based prediction of trajectories for socially compliant navigation," in *Proc. of Int. Conf. on Robotics: Science and Systems (RSS)*, 2012.
[14] D. Helbing and P. Molnár, "Social force model for pedestrian dynamics," *Physical Review E*, vol. 51, no. 5, pp. 4282–4286, May 1995.
[15] M. Luber, L. Spinello, J. Silva, and K. O. Arras, "Socially acceptable robot navigation: A learning approach." in *Proc. of The Int. Conf. on Intelligent Robots and Systems (IROS)*, 2012, pp. 902–907.
[16] P. Henry, C. Vollmer, B. Ferris, and D. Fox, "Learning to navigate through crowded environments," in *Robotics and Automation (ICRA), 2010 IEEE International Conference on*, may 2010, pp. 981 –986.
[17] Weinrich et al., "Estimation of human upper body orientation for mobile robotics using an svm decision tree on monocular images," in *Proc. Int. Conf. on Intel. Robots and Systems*, 2012, pp. 2147–2152.
[18] N. Dalal and B. Triggs, "Histograms of oriented gradients for human detection," in *Proc. of IEEE Int. Conf. on Computer Vision and Pattern Recognition (CVPR)*, 2005, pp. 886–893.
[19] K. Arras, O. Mozos, and W. Burgard, "Using boosted features for the detection of people in 2d range data," in *Proc. of Int. Conf. on Robotics and Automation (ICRA)*, 2007, pp. 3402 –3407.
[20] J. B. MacQueen, "Some methods for classification and analysis of multivariate observations," in *Proc. of the fifth Berkeley Symposium on Mathematical Statistics and Probability*, vol. 1, 1967, pp. 281–297.
[21] R. Philippsen and R. Siegwart, "An interpolated dynamic navigation function," in *Proceedings of the IEEE International Conference on Robotics and Automation (ICRA)*, 2005, pp. 3793 – 3800.
[22] K. Schenk, M. Eisenbach, A. Kolarow, and H.-M. Gross, "Comparison of laser-based person tracking at feet and upper-body height," in *Proc. of German Conf. on Advances in Artif. Intel. (KI)*, 2011, pp. 277–288.